

# Spectral properties of Co-decorated quasi 2-dimensional GaSe layer

I. Weymann,<sup>1,\*</sup> M. Zwierzycki,<sup>2,†</sup> and S. Krompiewski<sup>2</sup>

<sup>1</sup>*Faculty of Physics, Adam Mickiewicz University, 61-614 Poznań, Poland*

<sup>2</sup>*Institute of Molecular Physics, Polish Academy of Sciences, 60-179 Poznań, Poland*

(Dated: February 15, 2022)

Based on reliable *ab initio* computations and the numerical renormalization group method, systematic studies on a two-dimensional GaSe monolayer with a Co adatom have been carried out. It is shown that the stable lowest-energy configuration of the system involves the Co adatom located over Ga atom. For such configuration, it is demonstrated that the electronic and magnetic properties of the system can be effectively controlled by means of external factors, such as magnetic field, gate voltage or temperature. Moreover, if properly tuned, the GaSe-Co system can also exhibit the Kondo effect. The development of the Kondo phenomenon is revealed in the local density of states of the Co adatom, its magnetic field dependence, which presents the splitting of the Kondo peak, as well as in the temperature dependence of the conductance, which exhibits scaling typical of the spin one-half Kondo effect.

## I. INTRODUCTION

Two-dimensional (2D) and quasi two-dimensional monolayers have been recently intensively studied, both experimentally and theoretically, because they exhibit many remarkable physical phenomena, including mechanical, optoelectronic, electric and magnetic ones [1–6]. Moreover, it is now also well known that such systems can be additionally functionalized in various ways, e.g. by chemical doping [7], and by introducing either adatoms or vacancies and other defects [8–10]. In fact, the presence of magnetic adatoms can give rise to interesting strongly correlated phenomena, such as the Kondo effect [11, 12], which still, despite a few decades passed since its observation in artificial atoms [13], attracts a considerable attention [14–16]. Quite interestingly, the spectral signatures of adatoms placed on 2D materials have been analyzed in the Kondo regime in a number of works [17–21]. However, given a variety of 2D and quasi-2D materials, there are still some aspects that remain unexplored.

The system under consideration here is the GaSe monolayer with a unit cell composed of a Ga-Ga dimer covalently bonded to six Se atoms [7, 22]. Similar to many other low dimensional graphene-like layers, this material is also an object of particular interest. This is especially so because, in contrast to graphene, GaSe is a semiconductor with a pronounced energy gap—and can therefore serve as a transistor and possibly also as a promising material for solar energy harvesting [23]. In this paper we in particular focus on examining the spectral properties of GaSe monolayer decorated with Co adatoms. The analysis is performed by combining the first-principle calculations with the non-perturbative numerical renormalization group (NRG) method [24]. The *ab initio* computations are used to determine the density

of states of the system as well as the electron occupation and magnetic moment of the Co adatom. Then, the spectral properties of the adatom are determined by using NRG for an effective Anderson-like Hamiltonian. It is shown that the electronic and magnetic properties of the system can be tuned by external means, such as temperature, magnetic field or gate voltage. Furthermore, it is also demonstrated that the GaSe-Co system can exhibit the Kondo effect, if appropriately tuned.

## II. ELECTRONIC STRUCTURE AND EFFECTIVE MODEL

### A. First principles calculations

The electronic structure of the system was determined using the full potential linearized augmented plane wave method (FLAPW) [25] as implemented in the WIEN2K package [26]. In all the calculations the generalized gradient approximation (GGA) of density functional theory (DFT) was used with the exchange potential in the Perdew-Burke-Ernzerhof parametrization [27]. The integration over 2D Brillouin zone was performed using the mesh densities corresponding to several hundreds k-points (or more) with the convergence criteria for energy, charge per atom and forces set to  $10^{-4}$  Ry,  $10^{-3}$  e and 1 mRy/a.u., respectively. The GaSe monolayers were separated by 14 Å ensuring the lack of hopping between the neighboring planes.

The structure of GaSe monolayer, consisting of two atomic layers, is shown in Figs. 1(a)-(b). In the first step the lattice constant and the internal positions of 4 atoms within the unit cells were determined, the resulting parameters being  $a = 3.755$ ,  $d_{Ga-Ga} = 2.46$  and  $d_{Se-Se} = 4.85$  Å for the lattice constant and the distances between Ga and Se atoms, respectively. The calculated values are in good agreement with both the experimental data [28] and previous calculations [22]. The density of states (DOS) calculated for isolated monolayer is shown

\* weymann@amu.edu.pl

† maciej.zwierzycki@ifmpan.poznan.pl

in Fig. 1(c). The value of clearly observable band gap of  $\Delta = 2.1$  eV is close to previously calculated values [7, 22].

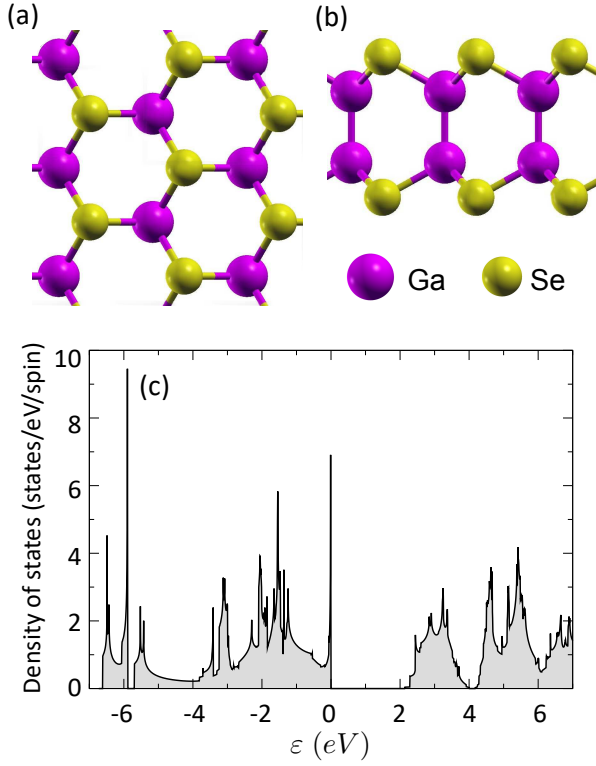


Figure 1. The structure of the GaSe monolayer as seen (a) from the top and (b) from the side. (c) The density of states of unadorned GaSe monolayer.

The case of GaSe monolayer with Co adatom was studied using  $3 \times 3$  supercell containing 37 atoms (18 Ga, 18 Se and one Co atom). Within the supercell, the size of which was fixed to the multiple of the previously determined values, the internal positions were fully relaxed. The place of most probable attachment of the adatom was determined by comparing the total energies for three high symmetry cases with Co positioned over Se, Ga and the center of the hexagon. These are indicated in Fig. 2(a), while the side views of the relaxed structures are shown in the panels (b)-(d) of the same figure. Visual analysis of the three structures suggests that the bonding strength is the weakest in the case of Co over Se [Fig. 2(b)] and the strongest for Co over Ga [Fig. 2(d)]. The Se-Co distance in the first case equals 2.46 Å. In the second case of centrally located adatom, its height over the plane of Se atoms is visibly smaller (1.27 Å). On the other hand, in the third case, Co over Ga, the adatom is actually embedded in the Se plane.

This conclusion is supported by a direct comparison of the total energy values, which stand in the following order

$$E_{Ga} < E_{center} < E_{Se},$$

with the lowest configuration being well separated from the other two ( $E_{center} - E_{Ga} \approx 6$  eV). In comparison, the

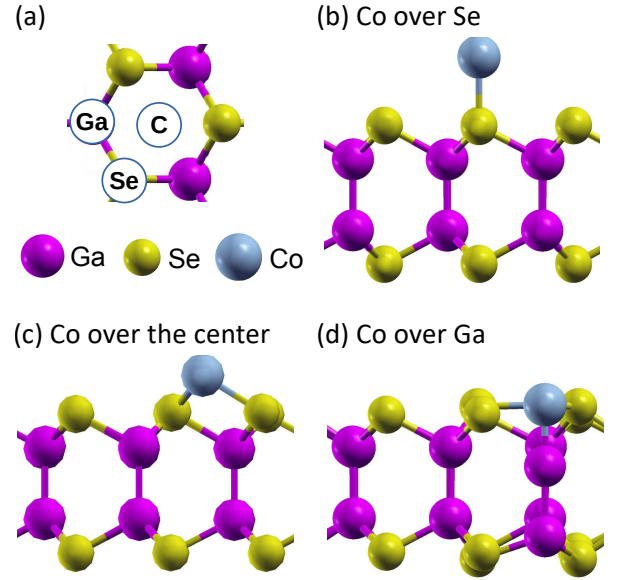


Figure 2. (a) Three possible positions of Co adatom – over Ga, Se and over the center of the hexagon (marked as C) – as seen from the top. (b)-(d) Side views of the cases from (a) (relaxed structures).

difference between the second and the third configuration energy is an order of magnitude smaller ( $E_{Se} - E_{center} \approx 0.7$  eV). The total magnetic moment, concentrated on the Co atom, ranges between atomic-like  $3\mu_B$  for the weakly bonded “Co over Se” geometry to the substantially reduced  $1\mu_B$  in the lowest energy case.

The density of states for the system with Co adatom, shown in Fig. 3(a) using red color, follows for the most part an outline of the density of states for clean GaSe (black line). The most visible differences between the two densities are located in the energy window corresponding to the clean case gap.<sup>1</sup> This is shown in Fig. 3(b) where in addition to the total DOS (red), the atomic contributions are also shown. The latter are, in the case of Se (green) and Ga (blue), summed over all the atoms of the given kind within the supercell. The highly localized states visible within the region of the GaSe gap are of almost pure Co- $d$  character (predominantly  $d_{x^2+y^2}$ ,  $d_{xy}$ ,  $d_{xz}$  and  $d_{yz}$ ), although certain level of hybridization with the surrounding atoms of the host can also be deduced.

In conclusion, the  $1\mu_B$  value of the magnetic moment coupled with its almost complete localization on adatom, suggests that the low-energy properties of the system under consideration can be correctly described using an effective spin- $\frac{1}{2}$  Anderson impurity model [29], as discussed in the following subsection.

<sup>1</sup> One notes that the Fermi energy of the Co-decorated system is anchored within the region of original gap because of the presence of the localized states discussed in the text.

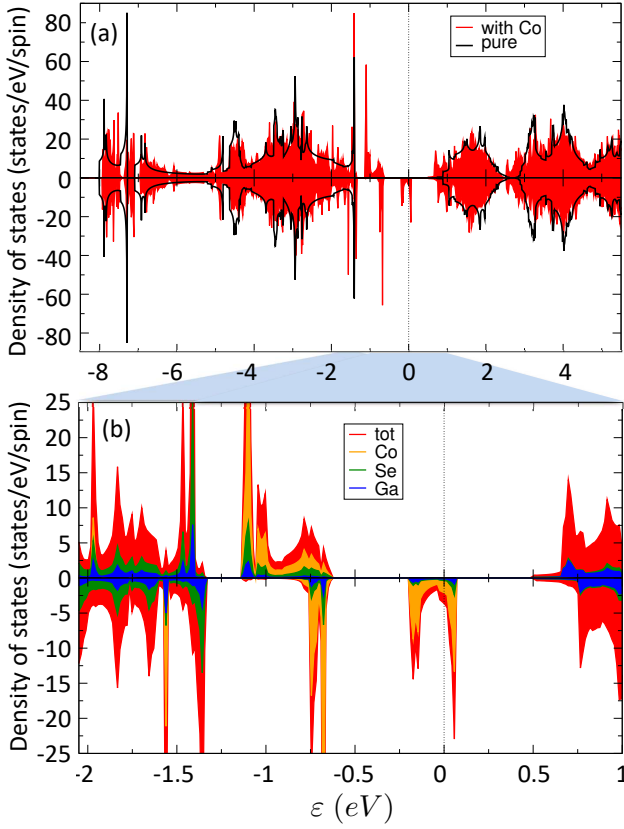


Figure 3. (a) The density of states for GaSe with Co adatom (red) together with the density of states of clean GaSe (black line). (b) The closeup of the behavior of the density of states around the Fermi energy, where the atomic contributions are also presented.

### B. Effective model

To obtain the most accurate results for the spectral properties of the Co adatom, we employ the density-matrix numerical renormalization group method [24, 30], developed originally by Wilson for the Kondo problem [12]. The effective Anderson-like model for the NRG computations has been constructed following the method described in Refs. [21, 31]. The crucial parameters of the Co adatom in this context are: the on-site Coulomb repulsion ( $U$ ), the level energy ( $\epsilon$ ), the hybridization parameter ( $V_{pd\sigma}$ ), and the Co  $d$ -shell occupancy ( $n_d$ ). The latter has been directly found from the *ab initio* calculations, to be equal to  $n_d = 7.6$ . The parameter  $U$  for Co is equal to 4 eV [8], whereas the hybridization has been found to be  $V_{pd\sigma} = -0.83$  eV by using the Harrison's scaling method [32] for the computed distances  $R_{CoGa} = 2.16$  Å (1st nearest neighbor) and  $R_{CoSe} = 2.33$  Å (2nd nearest neighbors). The charge states of the cobalt  $d$ -level correspond to energies [31]

$$E(j) = j\epsilon + Uj(j-1)/2 \quad (1)$$

with the minimum value for  $j_{min} \equiv n_d = 1/2 - \epsilon/U$ , i.e.  $\epsilon = -(n_d - 1/2)U$ .

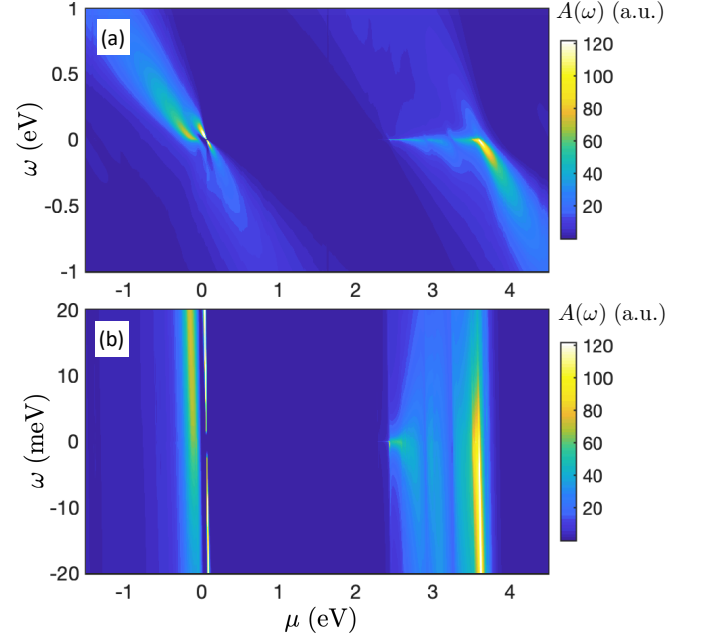


Figure 4. (a) The zero-temperature spectral function of the Co adatom calculated as a function of chemical potential  $\mu$ . (b) The low-energy behavior of the spectral function. The parameters of the effective Hamiltonian are  $\tilde{U} = 4$  eV,  $\tilde{\epsilon}_d = -0.4$  eV and hybridization  $V_{pd\sigma} = -0.83$  eV.

The energy separations of the relevant levels  $j = 7, 8, 9$  are  $\tilde{\epsilon}_d = E(8) - E(7)$  and  $2\tilde{\epsilon}_d + \tilde{U} = E(9) - E(7)$  and determine the parameters of the effective Anderson-like Hamiltonian. One then finds,  $\tilde{U} = U$ , and  $\tilde{\epsilon}_d = \epsilon + 7U = U(7.5 - n_d)$ . In calculations, we perform logarithmic discretization of the density of states of pure GaSe. Then, we tridiagonalize the discretized Hamiltonian by Lanczos method to obtain the hoppings and on-site energies along the Wilson chain [24]. In the next step, the eigenenergies and eigenvectors of the Hamiltonian are determined in an iterative fashion, which allow for determination of the density matrix and the relevant spectral operators. To perform computations, we have assumed the discretization parameter equal to  $\Lambda = 1.8$  and kept at least 1500 states at each iteration step. The quantity of interest is the spectral function  $A(\omega)$  of the adatom, which is defined as  $A(\omega) = -\text{Im}[G^R(\omega)]/\pi$ , where  $G^R(\omega)$  is the Fourier transform of the retarded Green's function of the adatom's effective orbital level.

### III. TRANSPORT PROPERTIES

The spectral function of Co adatom  $A(\omega)$  as a function of the chemical potential  $\mu$  and energy  $\omega$  is shown in Fig. 4(a), while the low-energy behavior of  $A(\omega)$  is displayed in Fig. 4(b). Because the density of states of pure GaSe exhibits a gap of the order of 2.1 eV, see Fig. 1(c), the spectrum has negligible weight at low-energies in the

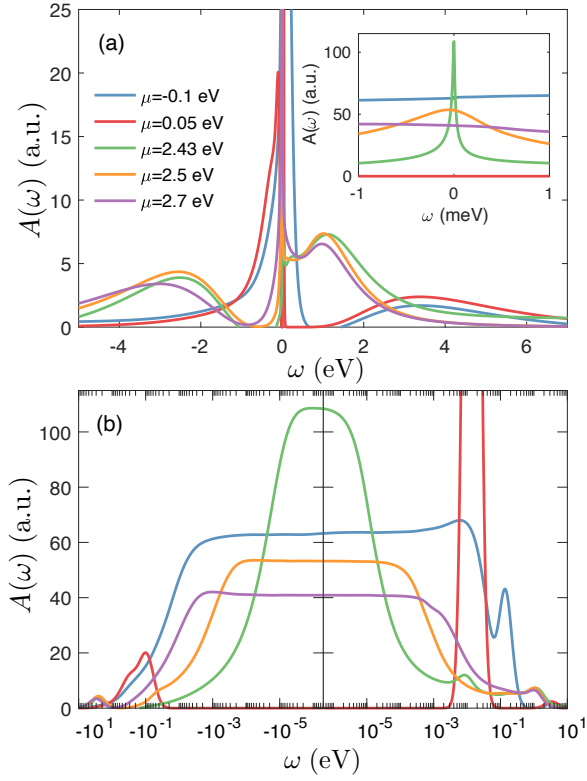


Figure 5. The spectral function for selected values of the chemical potential  $\mu$  plotted in the (a) linear and (b) logarithmic scale. The inset in (a) presents the low-energy behavior of the spectral function where a considerable Kondo peak is visible. The parameters are the same as in Fig. 4.

corresponding regime of  $0.2\text{eV} \lesssim \mu \lesssim 2.3\text{eV}$ . When the chemical potential is detuned out of this regime, the spectral function exhibits low-energy features resulting from strong correlations between the band electrons and the spin localized in the adatom's orbital. One of such phenomena is the Kondo effect, which manifests itself through a zero-energy resonance in the local density of states [11, 12]. Indications of such resonances can be clearly seen in Figs. 4(a)-(b).

Moreover, the low-energy behavior of Co adatom is also revealed in Fig. 5, which shows the energy-dependence of  $A(\omega)$  plotted both on the linear and logarithmic scale for selected values of the chemical potential. One can clearly identify the Hubbard resonances corresponding to  $\omega + \mu \approx \tilde{\epsilon}_d$  and  $\omega + \mu \approx 2\tilde{\epsilon}_d + \tilde{U}$ . Interestingly, for all considered values of  $\mu$ , except for  $\mu = 0.05\text{ eV}$ , there is a zero-energy resonance in the spectral function. This peak is clearly visible in the close-up on the low-energy behavior of  $A(\omega)$  shown in Fig. 5(a) as well as in the logarithmic-scale dependence presented in Fig. 5(b). Because for the selected values of chemical potential the adatom is mostly occupied by a single electron, one can conclude that the resonance is due to the Kondo effect. Here, however, one needs some care, since not all resonances need to be due to the Kondo correlations.

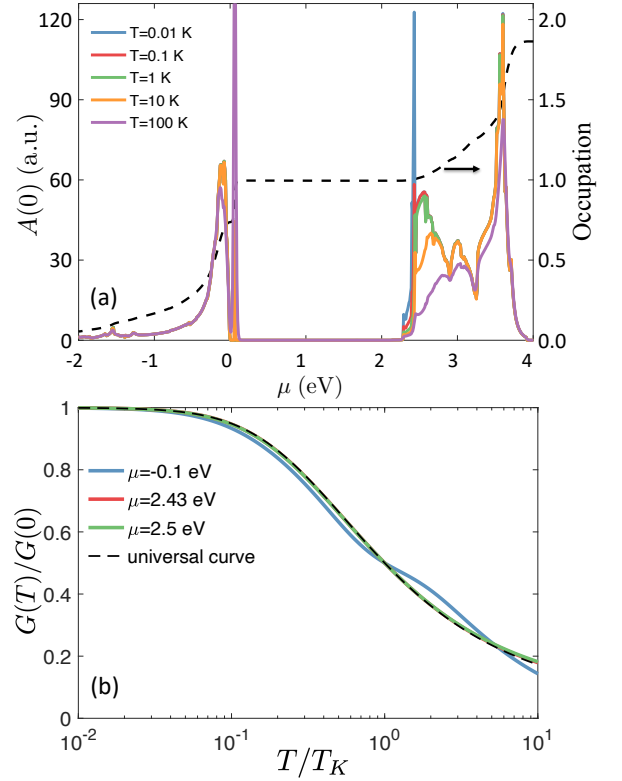


Figure 6. (a) The spectral function at the Fermi energy  $A(0)$  calculated for several values of temperature, as indicated. The dotted line presents the occupation of the adatom's orbital level. (b) The temperature dependence of the normalized linear conductance  $G(T)/G(0)$  calculated for selected values of the chemical potential as a function of the normalized temperature  $T/T_K$ . The dashed line presents the universal scaling plot for the spin-1/2 Kondo effect. The parameters are the same as in Fig. 4.

To shed more light on this issue, in Fig. 6(a) we present the chemical potential dependence of the spectral function taken at the Fermi energy  $A(0)$ . Because the Kondo resonance develops for temperatures  $T$  lower than the Kondo temperature  $T_K$ ,  $T \lesssim T_K$ , a strong dependence of  $A(0)$  on  $T$  can be observed for  $\mu \lesssim 0.2\text{ eV}$  and  $\mu \gtrsim 2.3\text{eV}$ . Nevertheless, as mentioned before, a special caution is needed since some low-energy features can be related to enhanced charge fluctuations around  $\mu \approx \tilde{\epsilon}_d$  and  $\mu \approx \tilde{\epsilon}_d + \tilde{U}$ . More specifically, the effects associated with Kondo correlations develop only in the local moment regime [12], i.e.  $\tilde{\epsilon}_d \lesssim \mu \lesssim \tilde{\epsilon}_d + \tilde{U}$ , where the adatom's occupation is odd, see the dotted line in Fig. 6(a). To understand the origin of the low-energy resonances, we have determined the linear response conductance at different temperatures, which would correspond to e.g. measuring the conductance over the Co adatom by STM. The normalized conductance in linear response can be found from [33]  $G(T)/G(0) = \int d\omega [-f'(w)] A(\omega)/A(0)$ , where  $f(\omega)$  denotes the Fermi-Dirac distribution function. In Fig. 6(b) we display the temperature dependence of



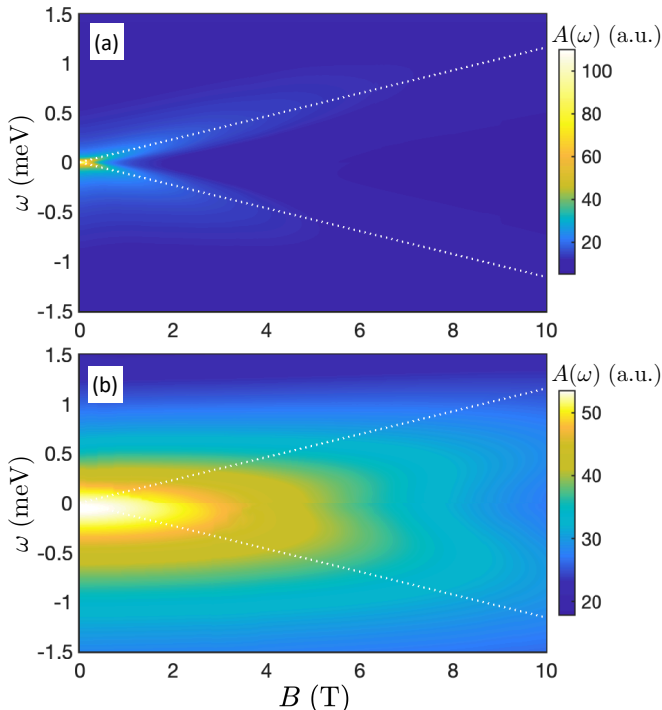


Figure 7. Spectral function plotted vs magnetic field demonstrating the splitting of the Kondo resonance for (a)  $\mu = 2.43$  eV and (b)  $\mu = 2.5$  eV. The parameters are the same as in Fig. 4 and the g-factor was assumed to be  $g = 2$ . The dotted lines indicate the Zeeman splitting energy  $\Delta_Z = g\mu_B B$ .

$G(T)/G(0)$  as a function of the normalized temperature  $T/T_K$ , where  $T_K$  is the Kondo temperature defined as temperature at which  $G(T) = G(0)/2$ . One can see that the resonances for  $\mu = 2.43$  eV and  $\mu = 2.5$  eV have the scaling characteristic of the Kondo effect— $G(T)/G(0)$  follows then exactly the universal scaling dependence of the spin-1/2 Kondo effect [12]. However,  $G(T)/G(0)$  in the case of  $\mu = -0.1$  eV does not match with the Kondo universal scaling and one can conclude that this resonance is not due to Kondo correlations, but rather associated with resonant charge fluctuations.

To corroborate our observations even more, in Fig. 7 we have determined the magnetic field dependence of the spectral function for two selected values of chemical potential, for which the temperature scaling of the conductance revealed the Kondo origin. Indeed, it can be clearly seen that the Kondo resonance becomes split by magnetic field and only side resonances at energies corresponding to the Zeeman energy  $\omega \approx \pm\Delta_Z$  are present,

where  $\Delta_Z = g\mu_B B$ , see the dotted lines in Fig. 7. Note also that in the case of  $\mu = 2.5$  eV a larger magnetic field is necessary to suppress and split the Kondo resonance, which is associated with larger Kondo temperature in this case compared to  $\mu = 2.43$  eV.

#### IV. CONCLUSIONS

In this paper we have investigated electronic and magnetic properties of the GaSe monolayer with a cobalt adatom. The focus has been put on the detailed analysis of local densities of states, spectral functions, and the possible Kondo resonances and their evolution with external magnetic field. The studies have been carried out in three steps by combining: (i) the first principles calculations, (ii) construction of an effective Anderson-type Hamiltonian, and (iii) the application of the numerical renormalization group. This allowed us for obtaining very accurate predictions for the spectral properties of Co-decorated quasi 2-dimensional GaSe layer.

In particular, the first-principle calculations provided the information about the lowest-energy configuration, the magnetic moment and occupation of the Co adatom. This information was further exploited to determine the parameters of the effective Hamiltonian and perform the NRG calculations. It turns out that the calculated local density of states of the Co adatom exhibits resonances depending on the position of the chemical potential. We have shown that these resonances can be associated with the Kondo correlations that develop between the adatom and two-dimensional host material. This observation has been corroborated by the analysis of the system's transport properties in external magnetic field and finite temperatures. In particular, the splitting of the Kondo peak in magnetic field as well as the Kondo universal scaling of the linear conductance have been demonstrated.

We believe that our study sheds more light on the spectral properties of magnetic adatom-decorated two dimensional materials and, especially, on the Kondo phenomena in such systems. The results show that the Co-decorated GaSe monolayer is an attractive Kondo system and its properties can be tuned by gate voltage or external magnetic field.

#### ACKNOWLEDGMENTS

I.W. acknowledges support by the Polish National Science Centre from funds awarded through the decision No. 2017/27/B/ST3/00621. The computing time at the Poznań Supercomputing and Networking Center is also acknowledged.

- 
- [1] Ashutosh Tiwari and Mikael Syväjärvi, *Advanced 2D Materials* (2016).
  - [2] Xiuling Li and Xiaojun Wu, “Two-dimensional monolayer

designs for spintronics applications,” *WIREs Comput. Mol. Sci.* **6**, 441–455 (2016).

- [3] K. S. Novoselov, A. Mishchenko, A. Carvalho, and

- A. H. Castro Neto, “2D materials and van der Waals heterostructures,” *Science* **353**, aac9439 (2016).
- [4] Phaedon Avouris, Tony F. Heinz, and Tony Low, *2D Materials: Properties and Devices* (Cambridge University Press, 2017).
- [5] Hamad Rahman Jappor, “Electronic structure of novel GaS/GaSe heterostructures based on GaS and GaSe monolayers,” *Physica B* **524**, 109–117 (2017).
- [6] Hamad Rahman Jappor and Majeed Ali Habeeb, “Optical properties of two-dimensional GaS and GaSe monolayers,” *Physica E* **101**, 251–255 (2018).
- [7] Ting Cao, Zhenglu Li, and Steven G. Louie, “Tunable magnetism and half-metallicity in hole-doped monolayer gase,” *Phys. Rev. Lett.* **114**, 236602 (2015).
- [8] T. P. Kaloni, N. Singh, and U. Schwingenschlög, “Prediction of a quantum anomalous hall state in co-decorated silicene,” *Phys. Rev. B* **89**, 035409 (2014).
- [9] L. Ao, H. Y. Xiao, X. Xiang, S. Li, K. Z. Liu, H. Huang, and X. T. Zu, “Functionalization of a gase monolayer by vacancy and chemical element doping,” *Phys. Chem. Chem. Phys.* **17**, 10737–10748 (2015).
- [10] Yihong Lu, Congming Ke, Mingming Fu, Wei Lin, Chunmiao Zhang, Ting Chen, Heng Li, Junyong Kang, Zhiming Wu, and Yaping Wu, “Magnetic modification of gase monolayer by absorption of single fe atom,” *RSC Adv.* **7**, 4285–4290 (2017).
- [11] J. Kondo, “Resistance minimum in dilute magnetic alloys,” *Prog. Theor. Phys* **32**, 37 (1964).
- [12] A. C. Hewson, *The Kondo problem to heavy fermions* (Cambridge University Press, Cambridge, 1997).
- [13] D. Goldhaber-Gordon, H. Shtrikman, D. Mahalu, D. Abusch-Magder, U. Meirav, and M.A. Kastner, “The Kondo effect in a single-electron transistor,” *Nature (London)* **391**, 156–159 (1998).
- [14] Gwangsu Yoo, S.-S. B. Lee, and H.-S. Sim, “Detecting Kondo Entanglement by Electron Conductance,” *Phys. Rev. Lett.* **120**, 146801 (2018).
- [15] Subhadeep Datta, Ireneusz Weymann, Anna Płomińska, Emmanuel Flahaut, Lætitia Marty, and Wolfgang Wernsdorfer, “Detection of Spin Reversal via Kondo Correlation in Hybrid Carbon Nanotube Quantum Dots,” *ACS Nano* **13**, 10029–10035 (2019).
- [16] Ivan V. Borzenets, Jeongmin Shim, Jason C. H. Chen, Arne Ludwig, Andreas D. Wieck, Seigo Tarucha, H.-S. Sim, and Michihisa Yamamoto, “Observation of the Kondo screening cloud,” *Nature* **579**, 210–213 (2020).
- [17] T. O. Wehling, A. V. Balatsky, M. I. Katsnelson, A. I. Lichtenstein, and A. Rosch, “Orbitally controlled Kondo effect of Co adatoms on graphene,” *Phys. Rev. B* **81**, 115427 (2010).
- [18] Victor W. Brar, Régis Decker, Hans-Michael Solowan, Yang Wang, Lorenzo Maserati, Kevin T. Chan, Hoonkyung Lee, Çağlar O. Girit, Alex Zettl, Steven G. Louie, Marvin L. Cohen, and Michael F. Crommie, “Gate-controlled ionization and screening of cobalt adatoms on a graphene surface,” *Nat. Phys.* **7**, 43–47 (2010).
- [19] Jindong Ren, Haiming Guo, Jinbo Pan, Yu Yang Zhang, Xu Wu, Hong-Gang Luo, Shixuan Du, Sokrates T. Pantelides, and Hong-Jun Gao, “Kondo Effect of Cobalt Adatoms on a Graphene Monolayer Controlled by Substrate-Induced Ripples,” *Nano Lett.* **14**, 4011–4015 (2014).
- [20] Damian Krychowski, Jakub Kaczkowski, and Stanislaw Lipinski, “Kondo effect of a cobalt adatom on a zigzag graphene nanoribbon,” *Phys. Rev. B* **89**, 035424 (2014).
- [21] I. Weymann, M. Zwierzycki, and S. Krompiewski, “Spectral properties and the Kondo effect of cobalt adatoms on silicene,” *Phys. Rev. B* **96**, 115452 (2017).
- [22] Yandong Ma, Ying Dai, Meng Guo, Lin Yu, and Baibiao Huang, “Tunable electronic and dielectric behavior of gas and gase monolayers,” *Phys. Chem. Chem. Phys.* **15**, 7098–7105 (2013).
- [23] Ashima Rawat, Raihan Ahammed, Dimple, Nityasagar Jena, Manish Kumar Mohanta, and Abir De Sarkar, “Solar energy harvesting in type ii van der waals heterostructures of semiconducting group iii monochalcogenide monolayers,” *The Journal of Physical Chemistry C* **123**, 12666–12675 (2019).
- [24] K. G. Wilson, “The renormalization group: Critical phenomena and the Kondo problem,” *Rev. Mod. Phys.* **47**, 773–839 (1975).
- [25] David Singh, *Planewaves, pseudopotentials, and the LAPW method* (Springer, New York, 2006).
- [26] P. Blaha, K. Schwarz, G. Madsen, D. Kvasnicka, and J. Luitz, *WIEN2k, An Augmented Plane Wave + Local Orbitals Program for Calculating Crystal Properties*, edited by Karlheinz Schwarz (Techn. Universität Wien, Austria, 2001).
- [27] John P. Perdew, Kieron Burke, and Matthias Ernzerhof, “Generalized gradient approximation made simple,” *Phys. Rev. Lett.* **77**, 3865–3868 (1996).
- [28] Xufan Li, Ming-Wei Lin, Alexander A. Puzdov, Juan C. Idrobo, Cheng Ma, Miaofang Chi, Mina Yoon, Christopher M. Rouleau, Ivan I. Kravchenko, David B. Geohegan, and Kai Xiao, “Controlled vapor phase growth of single crystalline, two-dimensional gase crystals with high photoresponse,” *Scientific Reports* **4** (2014), 10.1038/srep05497.
- [29] P. W. Anderson, “Localized magnetic states in metals,” *Phys. Rev.* **124**, 41 (1961).
- [30] Ö. Legeza, C.P. Moca, A.I. Tóth, I. Weymann, and G. Zaránd, “Manual for the flexible DM-NRG code,” arXiv:0809.3143v1 (2008), (the open access Budapest code is available at <http://www.phy.bme.hu/~dmnrg/>), <http://arxiv.org/abs/0809.3143v1>.
- [31] O. Újsághy, J. Kroha, L. Szunyogh, and A. Zawadowski, “Theory of the fano resonance in the stm tunneling density of states due to a single kondo impurity,” *Phys. Rev. Lett.* **85**, 2557 (2000).
- [32] Walter A. Harrison, *Electronic Structure and the Properties of Solids* (Dover Publications, New York, 1980).
- [33] Yigal Meir and Ned S. Wingreen, “Landauer formula for the current through an interacting electron region,” *Phys. Rev. Lett.* **68**, 2512–2515 (1992).